processes

MDPI

Article

Study on the Reservoir Heterogeneity of Different Volcanic Facies Based on Electrical Imaging Log in the Liaohe Eastern Sag

Zongli Liu [1,2], Huanping Wu [3], Shanyi Zhang [4] and Xiaoqing Zhao [5,*]

1 School of Earth Science, Northeast Petroleum University, Daqing 163318, China; liuzongli@nepu.edu.cn
2 Key Laboratory of Formation Mechanism and Resource Evaluation of Oil and Gas Reservoirs in Daqing, Daqing 163318, China
3 Office of Letters and Calls of Daqing, Daqing 163000, China
4 No. 5 Oil Production Plant PetroChina Daqing Oilfield Company, Daqing 163513, China
5 Institute of Unconventional Oil & Gas, Northeast Petroleum University, Daqing 163318, China
* Correspondence: zhaoxiaoqing@nepu.edu.cn

Abstract: The volcanic rocks of the Es3 Formation (the third member of the Eocene Shahejie) in the Liaohe Eastern Sag can be divided into four facies and twelve subfacies. The porosity spectrum, porosity bin, variation coefficient (VC), and porosity width derived from electrical imaging log data were applied to study and characterize the heterogeneity of four facies and nine subfacies, both qualitatively and quantitatively. However, the VC and porosity width cannot be used to quantitatively classify heterogeneity when the VC is small and the porosity width is large. In the present study, the authors propose a new parameter, P_{vcd} = variation coefficient × porosity width. Based on this parameter, using a combination of porosity spectra, porosity bin features, VC, and porosity width, lithofacies heterogeneity is divided into three categories. The first is weak heterogeneity, which has a $P_{vcd} < 1.1$, a VC < 0.15, and a porosity width < 6. The second is moderate heterogeneity, which has a P_{vcd} 1.1–1.6, a VC 0.15–0.25, and a porosity width 6–9. The third is strong heterogeneity, which has a $P_{vcd} > 1.6$, a porosity VC > 0.25, and a porosity width > 9. In these three cases, the porosity spectra mainly display unimodal features, the porosity bins are concentrated, the bimodal features with tails and porosity bins are less concentrated, or the multimodal features with tails and porosity bins are scattered, respectively. Favorable reservoirs of volcanic rocks are controlled by lithofacies. In the study area, the favorable reservoirs appear to be the diatreme subfacies with low or medium heterogeneity, the pyroclastic flow subfacies with low heterogeneity, the compound lava flow subfacies with low or medium heterogeneity, and the outer zone subfacies with strong heterogeneity.

Keywords: volcanic facies; heterogeneity; electrical imaging log; porosity spectrum

Citation: Liu, Z.; Wu, H.; Zhang, S.; Zhao, X. Study on the Reservoir Heterogeneity of Different Volcanic Facies Based on Electrical Imaging Log in the Liaohe Eastern Sag. *Processes* **2023**, *11*, 2427. https://doi.org/10.3390/pr11082427

Academic Editor: Qingbang Meng

Received: 27 July 2023
Revised: 9 August 2023
Accepted: 9 August 2023
Published: 11 August 2023

1. Introduction

Volcanic oil and gas reservoirs are widely distributed in many countries around the world. Recently, China found volcanic oil and gas reservoirs in Songliao, the Junggar, Sichuan, Liaohe, and many other basins which have great exploration prospects [1–4]. In recent years, significant progress has been made in the study of volcanic rock reservoirs, particularly in the identification of lithology and lithofacies, as well as their control effect on reservoirs [5–8]. Furthermore, analyses have been performed on the genetic relationship between pore evolution and the reservoir space, microscopic pore structures, the influences of alteration and diagenesis, and reservoir formation mechanisms [9–16]. These studies of volcanic rocks have great practical significance for oil and gas exploration. However, such studies have rarely used logging data to evaluate a crucial factor in volcanic reservoirs: heterogeneity. The heterogeneity of volcanic reservoirs affects the quality of reservoirs and the exploration and development of oil fields. Therefore, it is crucial to study the heterogeneity of volcanic rock reservoirs.

The methods often used in the study of volcanic reservoir heterogeneity include core observation, thin casting sections, scanning electron microscopy, conventional mercury injection, and constant-rate mercury injection [17–19]. These core experiments provide valuable and accurate results. However, due to the strong heterogeneity of volcanic rocks, the results of tests on rock cores cannot always reflect the pore characteristics of reservoirs [20,21]. Additionally, coring operations and the subsequent analyses are both expensive and time-consuming. Moreover, volcanic rock cores are fragile, which also increases the difficulty of testing. Previously, logging interpretation methods were used to quantitively study reservoir heterogeneity, mainly by using the permeability variation coefficient, abrupt injection coefficient, and gradient. However, these permeability parameters are usually not applicable because volcanic rock reservoirs are fractured, with significant changes in permeability [2,12]. Therefore, appropriate log data have been used to evaluate reservoir heterogeneity, with greater scientific significance and practical value. By contrast, electrical imaging log data have a high resolution and can reflect the distribution of reservoir pores. This method can clearly reflect the distribution information of pores and has continuity in the vertical direction; thus, it can accurately reflect the heterogeneity change characteristics of entire reservoirs. Moreover, the porosity spectrum and porosity bin obtained from electrical imaging logs can be applied to study pore structures and the development of reservoir pores [22–25]. Furthermore, they can indicate the level of heterogeneity [26–30]. In addition, researchers used electrical imaging data to study the influence of lithology on reservoir heterogeneity and classified this heterogeneity, confirming that this method can be applied in heterogeneity evaluation [31]. The heterogeneity of volcanic rock reservoirs is mainly controlled by volcanic facies and has little correlation with lithology. This work aimed to study the heterogeneity of different volcanic facies qualitatively and quantitatively in the Liaohe Eastern Sag and investigate the electrical imaging log responses. The porosity spectrum and bin, VC, and porosity width, as new parameters obtained from electrical imaging logs, are proposed to build a classification of volcanic facies heterogeneity. This comprehensive work helps to improve the evaluation of the heterogeneity of volcanic facies using well logs. Furthermore, the analysis of the heterogeneity characteristics of different volcanic facies can provide a more accurate basis for the study of reservoir laws and a reference for the evaluation of volcanic facies heterogeneity in other areas.

The Eastern Sag's lithology can be divided into basalt, non-dense basalt, trachyte, non-dense trachyte, diabase, and gabbro using logging data [5,32]. The volcanic rocks (excluding resedimented tuff, breccia, agglomerate and tuffaceous sandstone, and conglomerates) were divided into four facies and twelve subfacies according to the core, thin section, and logging data, and the abovementioned classification criteria were used [33]. These analyses laid the foundation for further research on heterogeneity in the Eastern Sag. Based on the lithofacies classification results, the heterogeneity of four facies and nine subfacies, which were widely distributed, was studied using electrical imaging log data, including volcanic conduit facies (diatreme), explosive facies (pyroclastic surge, pyroclastic flow), effusive facies (hyaloclastite, tabular flow, and compound lava flow), and extrusive facies (inner zone, middle zone, and outer zone). The aim of this work was to provide a reference for the subsequent development of volcanic reservoirs.

2. Geological Setting

The Eastern Sag is located in the eastern part of the Liaohe Depression, with a northeast strike on the plane. It is located in the Tanlu Fault zone, with frequent tectonic movement and strong fault activity. Influenced by the Tanlu Fault zone, a series of NE-trending faults have developed, such as the Jiazhangsi fault and Jiadong fault (Figure 1). The Jiazhangsi fault is located in the center of the basin and is the longest and most important fault running through it. Since the Cenozoic era, frequent volcanic activities have led to the widespread development of volcanic rocks with trachyte, basalt, and diabase (Table 1). The Shahejie Formation period is the strongest and most representative, resulting in the widespread distribution of volcanic rocks. The distribution range of volcanic rocks is clearly controlled

by faults and is limited by the fault system. The thickness near the main fault (Jiazhangsi Fault) is the greatest, gradually thinning towards both sides. Volcanic rocks with a thickness exceeding 1 km are usually less than 2 km away from the main fault. Accordingly, the research wells are all located near the fault, and Es3 was selected as the study strata.

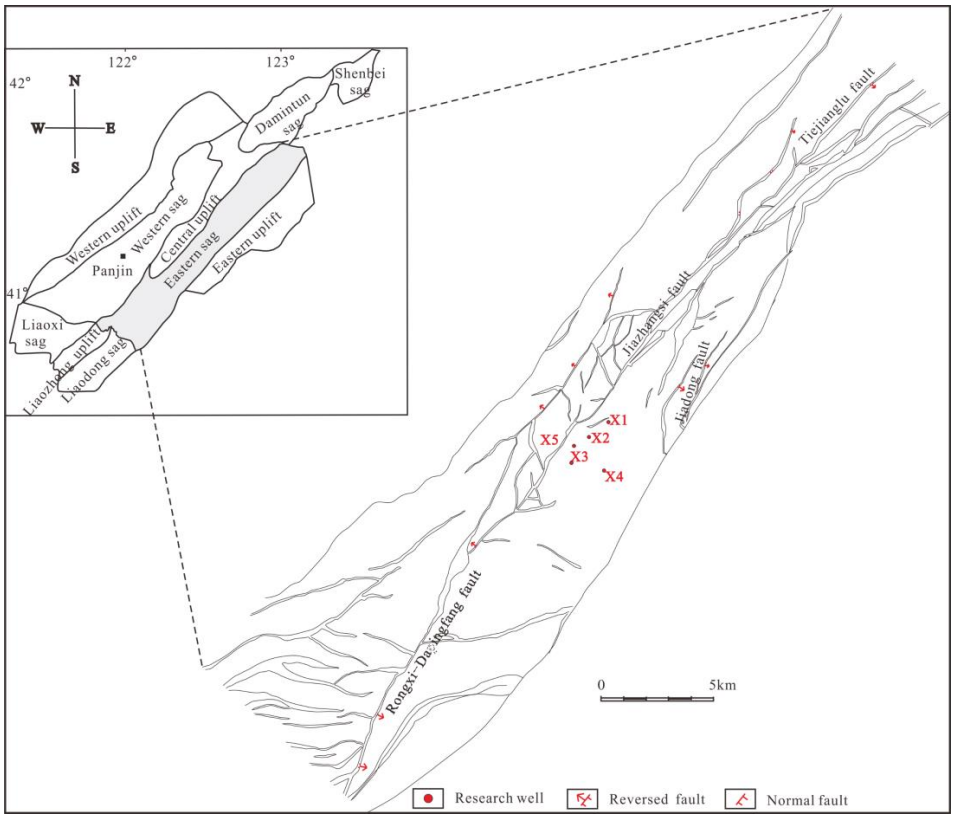

Figure 1. Structural distribution map and distributions of research wells in the Eastern Sag.

Table 1. Stratigraphic and lithological characteristics of the Paleogene in the Liaohe Basin.

Geological Period		Strata			Lithology
		Formation	Member	Symbol	
Paleogene	Oligocene	Dongying	first	Ed1	basalt
			second	Ed2	Basalt and trachyte
			third	Ed3	basalt
	Eocene	Shahejie	first	Es1	basalt
			second	Es2	Basalt and diabase
			third	Es3	basalt, trachyte, and diabase
			fourth	Es4	basalt, basaltic sedimentary tuff, and tuffaceous sandstone
	Paleocene	Fangshenpao	upper	Efu	basalt
			lower	Efl	Basalt and tuffaceous sandstone

3. Materials and Methods

3.1. Materials

The electrical imaging log data of 5 wells were used, derived from the Es3 Formation in the Eastern Sag of the Liaohe Basin. The electrical imaging log data were obtained using a Haliburton's X-tended Range Micro Imager (XRMI), and the detection depth was the

flushing zone. The tool, with a high resolution of 2 inches, has 150 independent electrodes which measure variations in electrical current [29,32]. These variations in current can reflect the resistivity of the formation. Certain parameters representing heterogeneity can be obtained after processing. Well X1 can be used to study the heterogeneity of the diatreme, as well as the pyroclastic surge and pyroclastic flow subfacies. Well X2 can be used to study the heterogeneity of the compound lava flow subfacies. Well X3 can be used to study the heterogeneity of the hyaloclastite subfacies. Well X4 can be used to study the heterogeneity of the tabular flow subfacies. Well X5 can be used to study the heterogeneity of the inner zone, middle zone, and outer zone subfacies.

3.2. Methods

3.2.1. Resistivity Calibration

The button electrode of the electrical imaging log measures the resistivity value of the scanned formation [25,34]. Due to the dynamic adjustment of the current during the measurement process, the conductivity value cannot truly reflect the absolute change in the formation's resistivity. Therefore, it needs to be rewritten and expressed as the resistivity value. Based on a previous study [31,35], R_{LLS} (shallow lateral resistivity) was selected to calibrate the conductivity of the electrical imaging log:

$$R_i = \frac{\overline{\sigma}}{\sigma_i} R_{LLS} \tag{1}$$

where R_i is the resistivity value of the i button electrode, Ω·m; σ_i is the conductivity value of the ith button, S/m; $\overline{\sigma}$ is the average value of all the conductivities at each sampling depth point, S/m; and R_{LLS}, Ω·m.

3.2.2. Porosity Calibration

The detection depth of the electrical imaging log is equivalent to R_{LLS}, which is the range of the flushing zone around the wellbore [5,35]. According to the classic Archie formula,

$$\varphi^m R_{xo} = \frac{abR_{mf}}{S_{xo}^n} \tag{2}$$

where a and b are lithologic coefficients; m is the cementation index; n is the saturation index; R_{xo} is the resistivity of the flushed zone, Ω·m; S_{xo} is the water saturation; φ is the porosity; and R_{mf} is the mud resistivity, Ω·m.

By substituting the calibrated R_i for R_{xo}, the corresponding porosity becomes φ_i. Using R_{LLS} as R_{xo}, the corresponding porosity is φ_e (the effective porosity). By substituting Equation (2), we obtain

$$\varphi_i^m R_i = \varphi_e^m R_{LLS} \tag{3}$$

According to Equations (1) and (3), the corresponding porosity value of each button can be obtained as follows:

$$\varphi_i = \sqrt[m]{\frac{\sigma_i}{\overline{\sigma}}} \times \varphi_e \tag{4}$$

where φ_i is the porosity calculated from the electrical imaging log.

Due to the omission of the Archie formula calculation step in Equation (4) and the elimination of the influences of a, b, m, and multiple wellbore parameters, only the cementation index m remains, effectively improving the adaptability and computational accuracy [22,27,31,32].

3.2.3. Porosity Spectra, Porosity Bins, Porosity Variation Coefficient, and Porosity Width

After the resistivity calibration, porosity calibration, and the acquisition of frequency statistics, the electrical imaging log data can form a frequency distribution spectrum of porosity (Figure 2). The number of peaks and the width and tail of the porosity spectrum

can qualitatively characterize heterogeneity. The more peaks there are, the larger the width, the longer the tail, and the stronger the heterogeneity is [32].

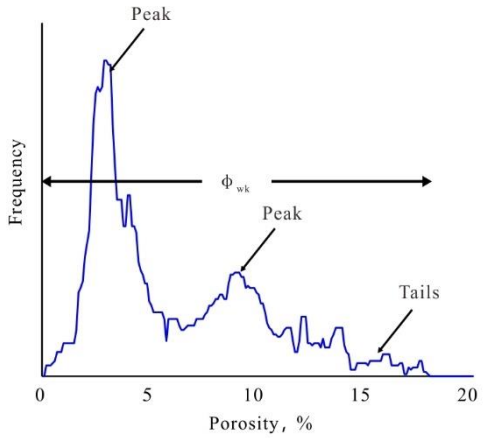

Figure 2. Characteristics of porosity spectrum and parameters.

The cumulative porosity data "PS3, PS5, PS7, …, PS50" represent porosity values of "≤0.03, 0.05, 0.07, …, ≤0.5", etc., and the porosity bins were obtained, as shown by the various colors in the seventh track in Figure 3. On the basis of the number and concentration of porosity bins, reservoir heterogeneity can be qualitatively analyzed [20,21,32]. The more porosity bins there are, the more scattered the pores are, and the stronger the heterogeneity is. For example, at 4574–4580 m, in Figure 3, the porosity bins show that PS7–PS10 accounted for more than 75%, indicating weak heterogeneity.

In order to quantitatively evaluate the heterogeneity of different facies, the VC and porosity width were extracted based on the porosity spectrum.

The VC is obtained as

$$\phi_{VK} = \frac{\sigma_\varphi}{\overline{\varphi}} \tag{5}$$

$$\sigma_\varphi = \sqrt{\frac{\sum_{i=1}^{n} (\varphi_i - \overline{\varphi})^2}{n}}$$

where ϕ_{VK} is the VC; σ_φ is the porosity standard deviation; $\overline{\varphi}$ is the average porosity; and n is the total number of porosity bins. A larger VC is indicative of stronger heterogeneity. The authors previously divided volcanic rocks into three categories of heterogeneity using the VC and other parameters, with VC < 0.15 (I), 0.15–0.25 (II), and >0.25 (III) [31].

The porosity width (Figure 2) is obtained as

$$\phi_{WK} = \varphi_{\max} - \varphi_{\min} \tag{6}$$

where ϕ_{WK} is the porosity width, and $\varphi_{\max}$ and $\varphi_{\min}$ are the maximum and minimum porosity values in the fixed window length. A larger porosity width is indicative of stronger heterogeneity.

The VC and porosity width of the same subfacies vary greatly, which implies a scattered porosity distribution and strong longitudinal heterogeneity.

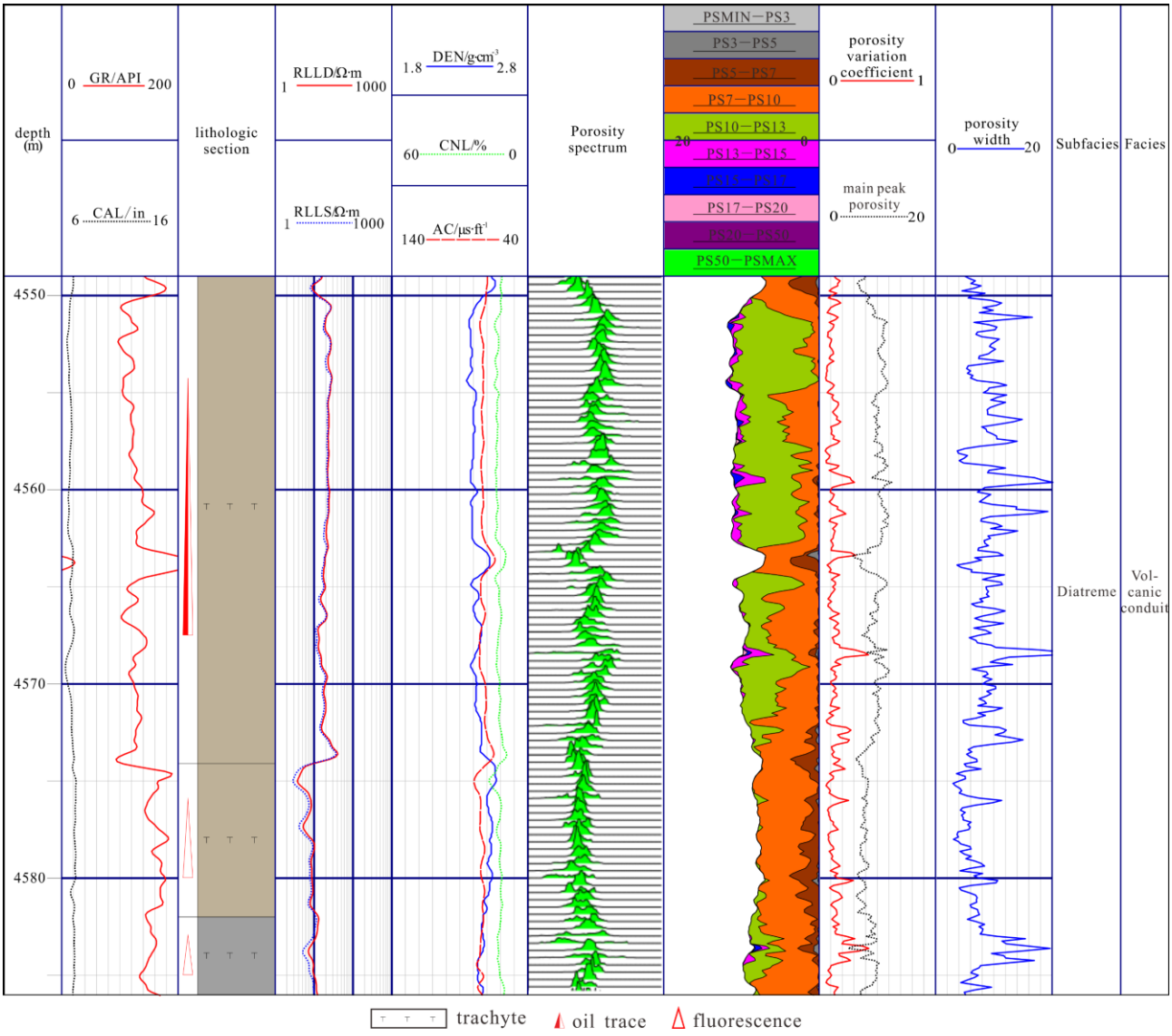

Figure 3. Heterogeneity characteristics of the diatreme in subfacies Well X1.

4. Results

4.1. Heterogeneity Characteristics of Diatreme Subfacies in Volcanic Conduit Facies

The lithology of the 4550–4580 m section in Well X1 was trachyte, and the lithofacies was determined to be a diatreme subfacies. The mud logging showed oil traces and fluorescence (Figure 3). The porosity spectra were mainly displayed in a unimodal distribution. The porosity bins were concentrated. The VC showed low values, and the porosity width showed moderate values. These findings indicate that the pores in the diatreme subfacies are relatively evenly distributed, with weak–moderate vertical and horizontal heterogeneity.

The porosity analysis results indicated that most of the spectra displayed a narrow unimodal distribution without tails except for some intervals (4564–4573 m) that showed a bimodal distribution with tails (Figure 3). This hints that the porosity was concentrated. The porosity bins at the 4550–4563 m interval showed that PS10–PS13 had over 80% porosity, and the main peak porosity was approximately 10.5%, which is within the porosity bin. The porosity bins at the 4574–4580 m interval showed that PS7–PS10 had over 75% porosity, and the main peak porosity was approximately 7.7%, which is also within the porosity bin. These results showed that the pores were uniformly distributed and concentrated in the

longitudinal direction, leading to weak vertical and horizontal heterogeneity. The VC was approximately 0.13, showing a low value, while the porosity width was approximately 8.6, showing a moderate value. Moreover, the VC curve displayed a mostly micro-tooth shape in the longitudinal direction; however, the width curve mostly exhibited high-amplitude serration. These findings indicate a weak–moderate vertical and horizontal heterogeneity of the diatreme subfacies.

4.2. Heterogeneity Characteristics of Explosive Facies

4.2.1. Heterogeneity Characteristics of Pyroclastic Surge Subfacies in Explosive Facies

The lithology of the 4040–4065 m interval in Well X1 was trachytic tuff, and the lithofacies was determined to be a pyroclastic surge subfacies. The mud logging showed fluorescence (Figure 4). The porosity spectra were mainly displayed in a unimodal distribution with tails. The porosity bins were concentrated. The VC showed low values, and the porosity width showed moderate values. These findings indicate that the pores in the pyroclastic surge subfacies are relatively evenly distributed, with weak vertical and horizontal heterogeneity.

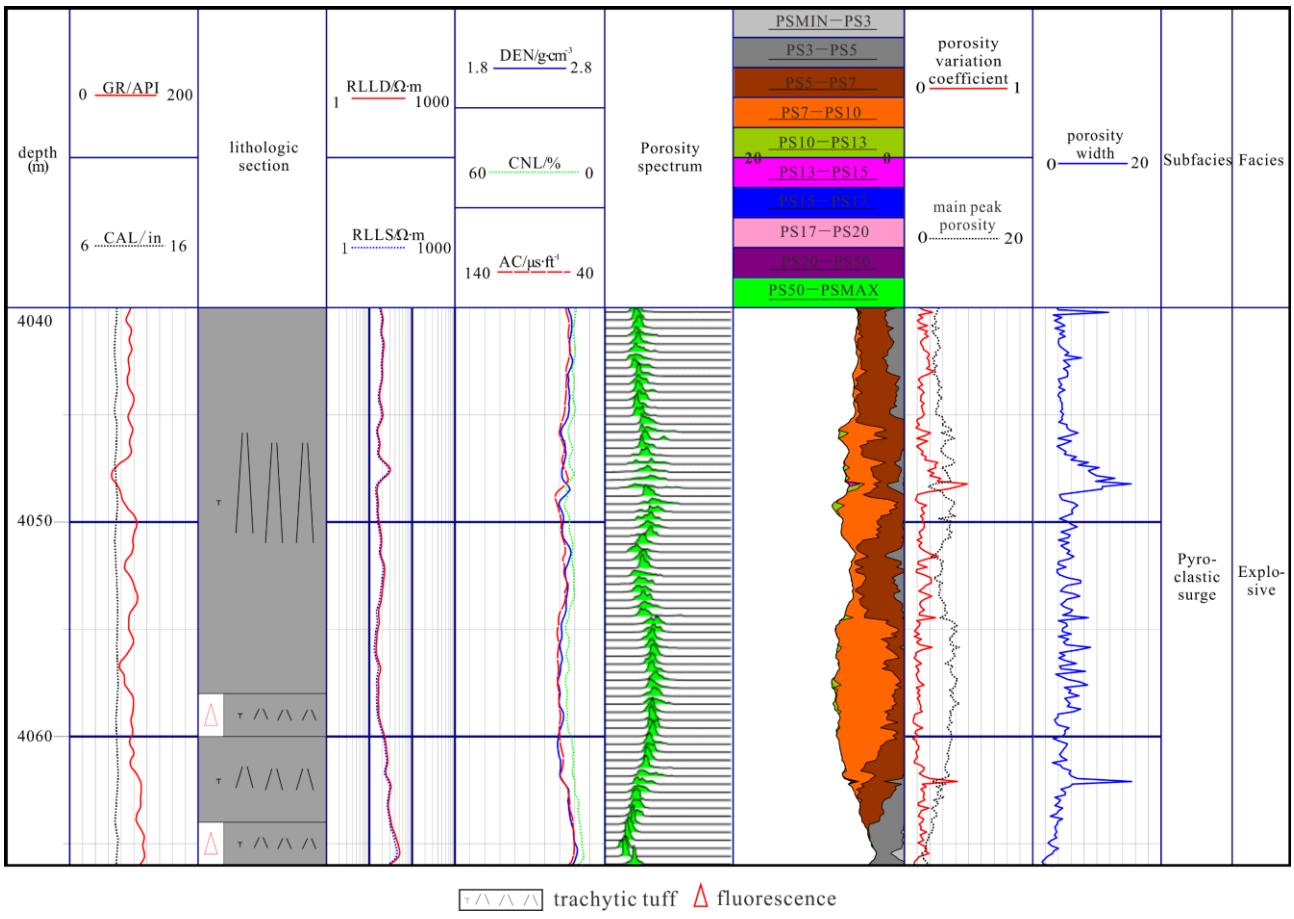

Figure 4. Heterogeneity characteristics of pyroclastic surge subfacies in Well X1.

The porosity analysis results indicated that most of the spectra displayed a narrow unimodal distribution with tails (Figure 4). This hints that the porosity was concentrated. The porosity bins (4040–4045 m, 4051–4054 m) showed that PS5–PS7 had over 80% porosity, and the main peak porosity was approximately 5.6%, which is within the porosity bin. The porosity bins at the 4054–4062 m interval showed that PS7–PS10 had over 80% porosity, and the main peak porosity was approximately 7.3%, which is also within the porosity bin. These results indicated that the pores were uniformly distributed and concentrated in the

longitudinal direction, leading to weak vertical and horizontal heterogeneity. The VC was approximately 0.144, and the porosity width was approximately 5.3, both showing low values. Moreover, the VC curve mostly showed micro-fluctuations in the longitudinal direction; however, the width curve mostly showed low-amplitude serration. These findings reflect the weak vertical and horizontal heterogeneity of the pyroclastic surge subfacies.

4.2.2. Heterogeneity Characteristics of the Pyroclastic Flow Subfacies in Explosive Facies

The lithology of the 4450–4478 m interval in Well X1 was trachyte, and the lithofacies was determined to be a pyroclastic flow subfacies. The mud logging showed oil traces and oil patches (Figure 5). The porosity spectra were mainly displayed in a unimodal distribution. The porosity bins were concentrated in the PS10–PS13 range. The VC showed low values, and the porosity width showed moderate values. These findings indicate that the pores in the pyroclastic flow subfacies are relatively evenly distributed, with weak–moderate vertical and horizontal heterogeneity.

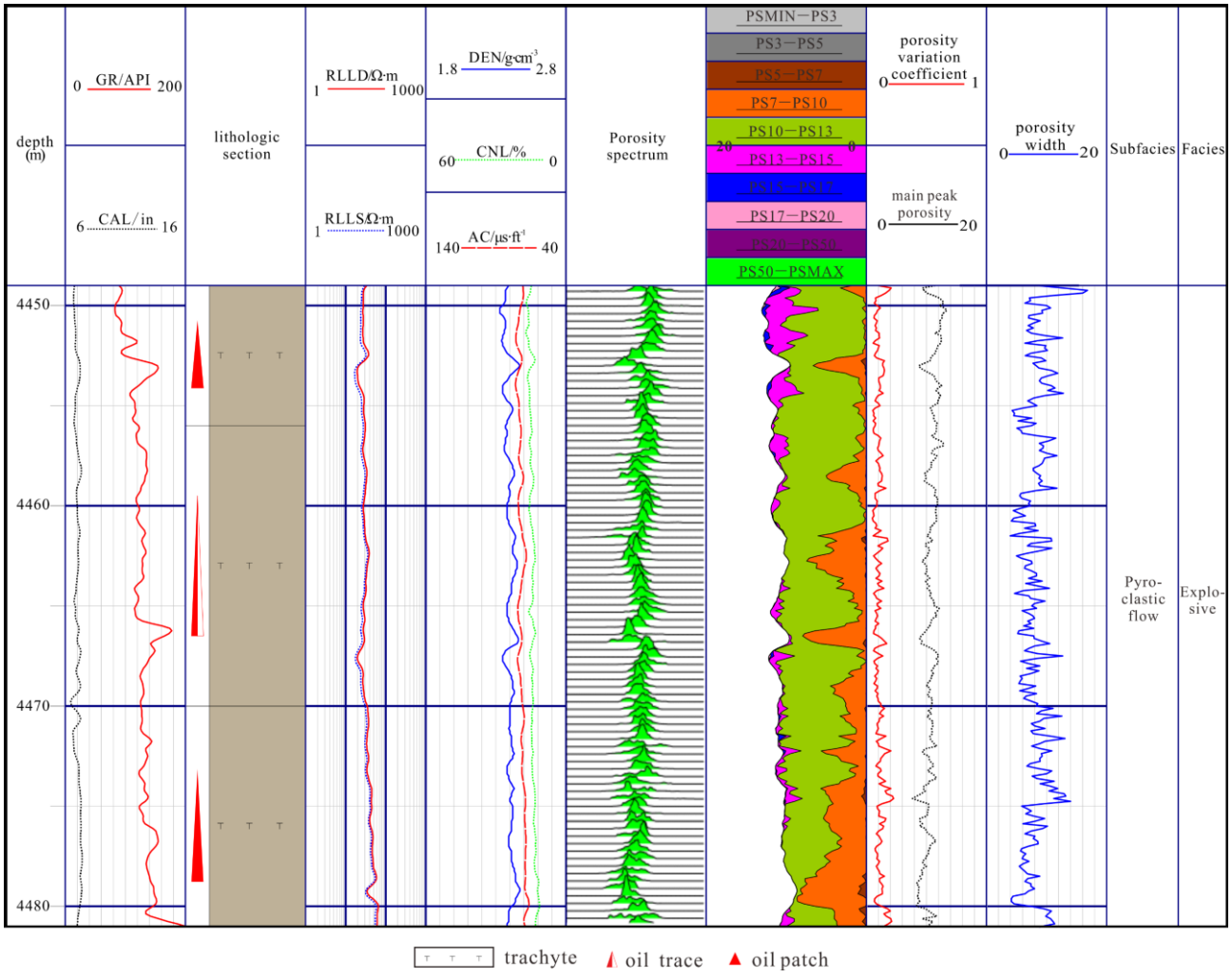

Figure 5. Heterogeneity characteristics of pyroclastic flow subfacies in Well X1.

The porosity analysis results indicated that the vast majority of the spectra were characterized by narrow, unimodal behavior without tails (Figure 5). This hints that the porosity was concentrated. The porosity bins showed that PS10–PS13 had over 80% porosity, and the main peak porosity was approximately 10.9%, which is within the porosity bin. These results showed that the pores were uniformly distributed and concentrated in the longitudinal direction, leading to weak vertical and horizontal heterogeneity. The

VC was approximately 0.104, showing a low value; the porosity width was approximately 8.2, showing a moderate value. Moreover, the VC and main peak porosity curves mostly exhibited a micro-tooth shape and were nearly smooth in the longitudinal direction; however, the width curve mostly showed low-amplitude serration. These findings indicate the weak–moderate vertical and horizontal heterogeneity of the pyroclastic flow subfacies.

4.3. Heterogeneity Characteristics of Effusive Facies

4.3.1. Heterogeneity Characteristics of Hyaloclastite Subfacies in Effusive Facies

The lithology of the 3802–3836 m interval in Well X3 was basalt, and the lithofacies was determined to be a hyaloclastite subfacies. The mud logging indicated oil patches and oil traces (Figure 6). The porosity spectra were mainly displayed in a broad, bimodal distribution with tails. The porosity bins were diverse. The VC showed moderate values, and the porosity width showed high values. These findings indicate that the reservoir in the hyaloclastite subfacies was developed, with a relatively dispersed pore distribution and moderate–strong vertical and horizontal heterogeneity.

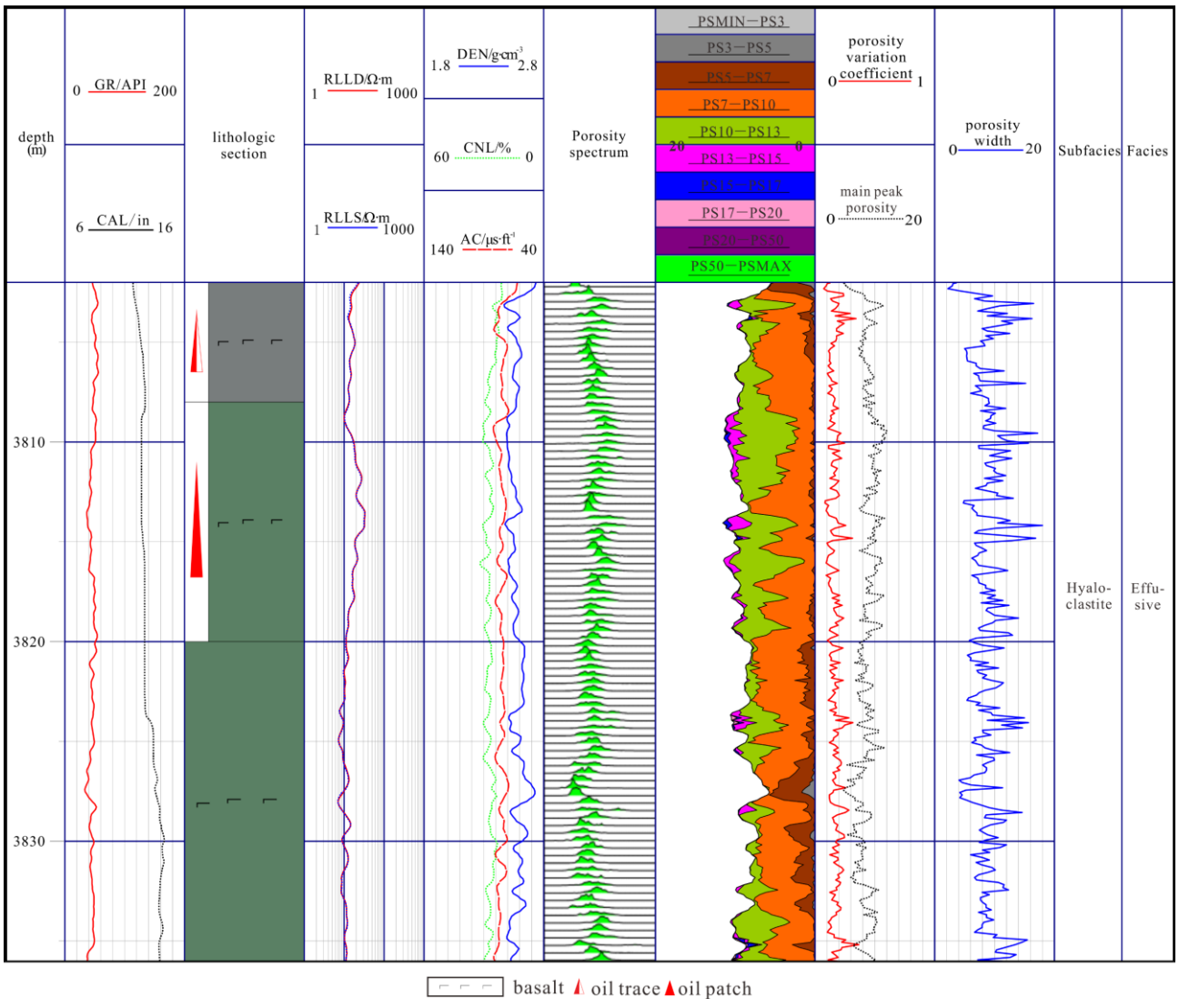

Figure 6. Heterogeneity characteristics of hyaloclastite subfacies in Well X3.

The porosity spectra analysis results indicated that most cases were characterized by a broad, bimodal spectrum with tails (Figure 6). This hints that the porosity was less concentrated. The porosity at the 3802–3835 m interval reflected a variety of porosity

bins, and the main peak porosity had a multi-fingered feature. These results showed that the pores were not concentrated in the longitudinal direction, leading to relatively strong vertical and horizontal heterogeneity. The VC was approximately 0.166, showing a moderate value; the porosity width was approximately 9.0, showing a high value. Moreover, the VC curve displayed a mostly micro-tooth shape in the longitudinal direction; however, the width curve mostly showed a high-amplitude tooth shape and multi-fingering. These findings indicate the moderate–strong vertical and horizontal heterogeneity of the hyaloclastite subfacies.

4.3.2. Heterogeneity Characteristics of Tabular Flow Subfacies in Effusive Facies

The lithology of the 3825–3845 m interval in Well X4 was basalt, and the lithofacies was determined to be a tabular flow subfacies. The mud logging indicated fluorescence (Figure 7). The porosity spectra were mainly displayed in a bimodal distribution with tails. The porosity bins were less concentrated. The VC and porosity width showed moderate values. These findings indicate that the pores in the tabular flow subfacies are relatively evenly distributed, with moderate vertical and horizontal heterogeneity.

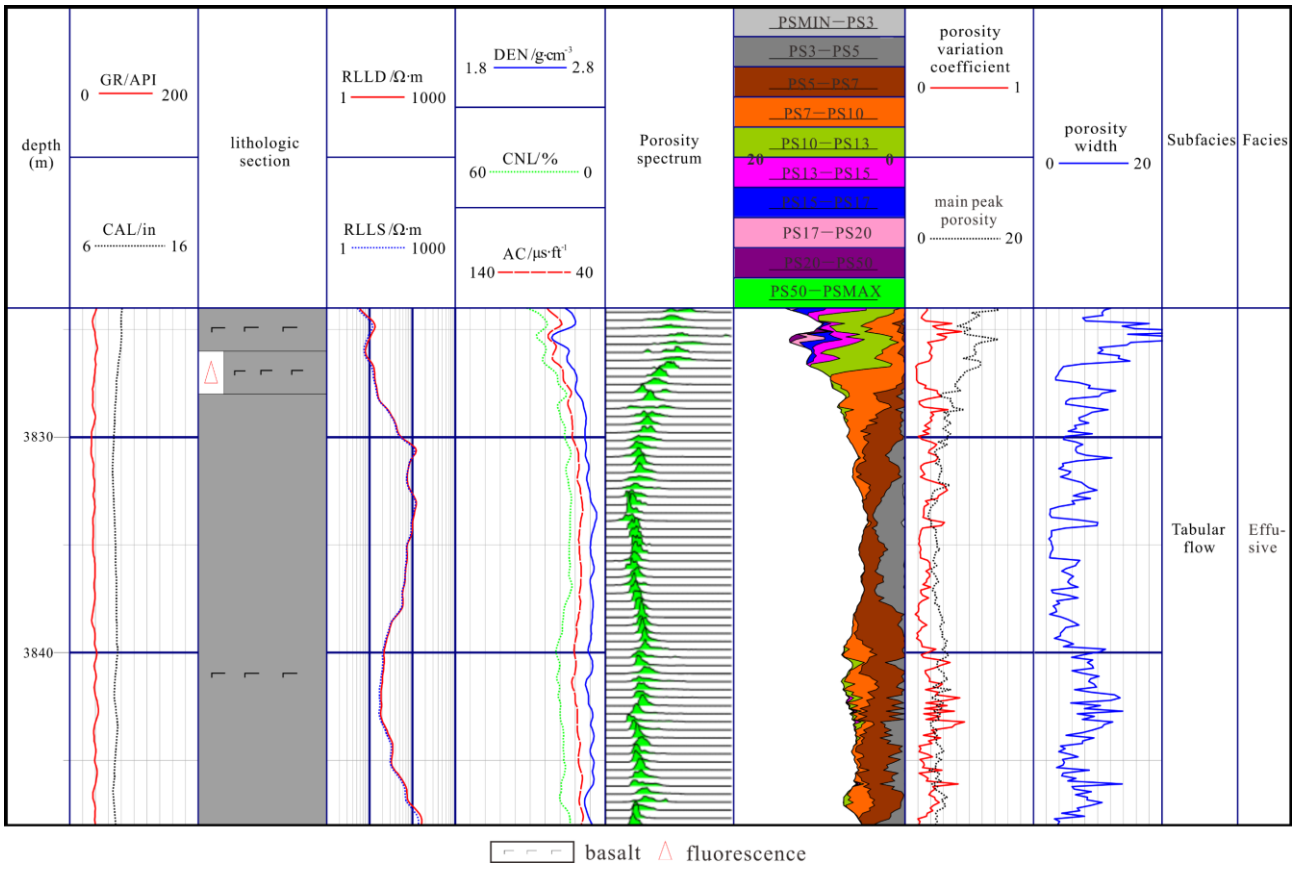

Figure 7. Heterogeneity characteristics of tabular flow subfacies in Well X4.

The tabular flow subfacies reservoir can be divided into two parts: the top and bottom parts with developed pores and the middle part with dense blocks. The average porosity of the top part (3825–3832 m) with developed pores was approximately 8.4%. The results of the porosity spectra analysis revealed that the vast majority of cases were characterized by very broad, multimodal behavior with tails (Figure 7). This implies dispersed pores. The VC was approximately 0.19, a moderate value; the porosity width was approximately 9.6, a high value. Furthermore, the VC, main peak porosity, and porosity width curves had a mostly high-amplitude tooth shape in the longitudinal direction. This indicates

moderate–strong vertical and horizontal heterogeneities in the top part of the tabular flow subfacies.

The average porosity of the middle part (3833–3838 m) with dense blocks was approximately 4.9%. The results of the porosity spectra analysis showed that most cases were characterized by a narrow, unimodal distribution with tails. The porosity bins showed that PS3–PS5 had a porosity of over 60%, and the main peak porosity was approximately 4.5%, which is within the porosity bin. These results indicated that the pores were uniformly distributed and concentrated in the longitudinal direction, leading to weak vertical and horizontal heterogeneity. The VC was approximately 0.15, and the porosity width was approximately 4.5, showing low values. Moreover, in the longitudinal direction, the VC and main peak porosity curves showed a mostly micro-tooth shape and were nearly smooth. This indicates weak vertical and horizontal heterogeneity in the middle part of tabular flow subfacies.

4.3.3. Heterogeneity Characteristics of Compound Lava Flow Subfacies in Effusive Facies

The lithology of the 3511–3540 m interval in Well X2 was basalt, and the lithofacies was determined to be a compound lava flow subfacies. The mud logging indicated fluorescence (Figure 8). The porosity spectra were mostly characterized by a very broad, multimodal spectrum with tails. The porosity bins were diverse. The VC showed moderate values, and the porosity width showed high values. These findings indicate that the reservoir in the compound lava flow subfacies was developed, with a relatively dispersed pore distribution and moderate–strong vertical and horizontal heterogeneity.

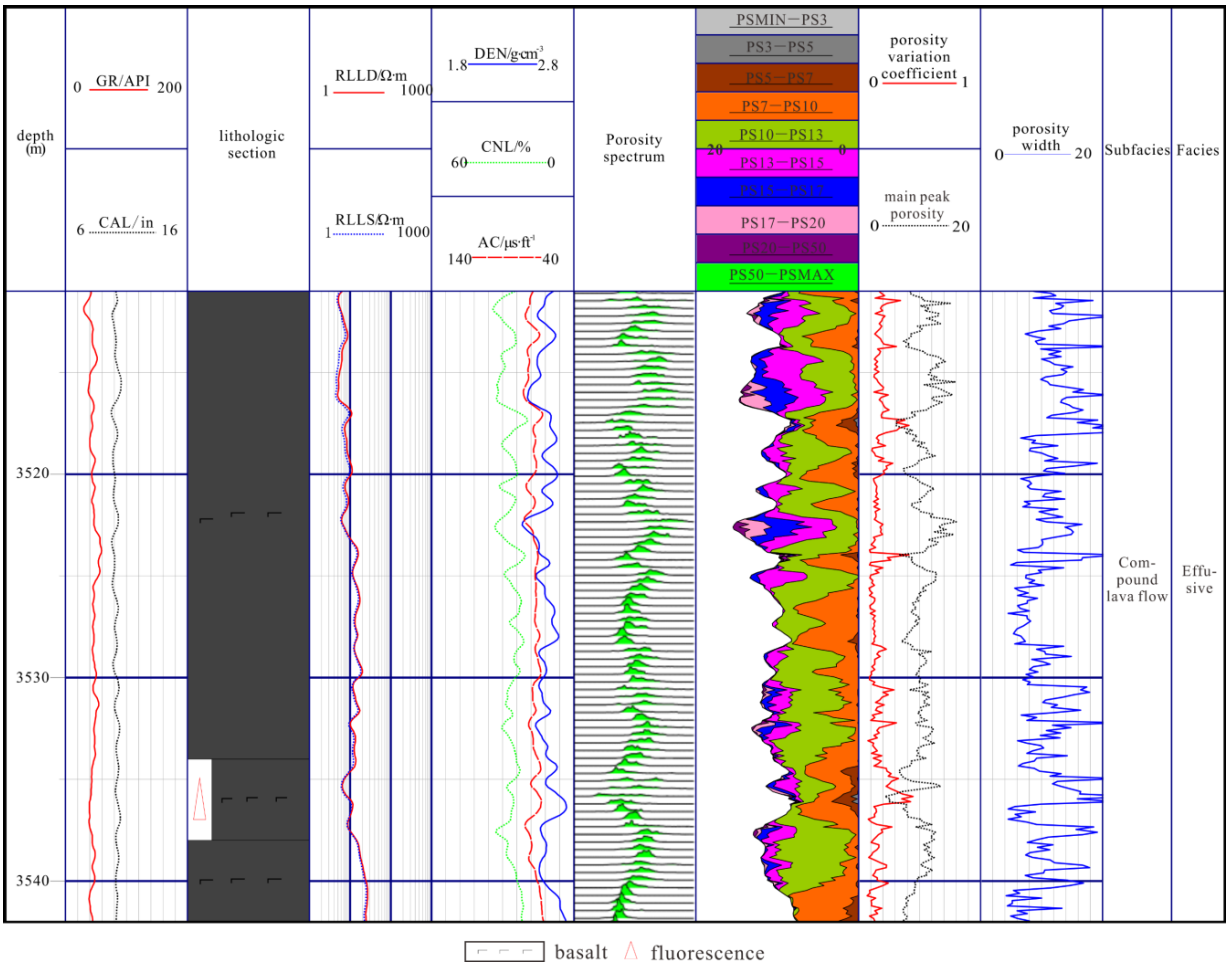

Figure 8. Heterogeneity characteristics of compound lava flow subfacies in Well X2.

The porosity spectra analysis results showed that most cases were characterized by a very broad, multimodal spectrum with tails (Figure 8). This implies dispersed porosity. The porosity interval was observed in a variety of porosity bins, and the main peak porosity had a multi-fingered feature. These results indicated that the pores were not concentrated, leading to relatively strong vertical and horizontal heterogeneity. The VC was approximately 0.171, a moderate value; the porosity width was approximately 11.4, a high value. Moreover, the VC curve mostly displayed a low tooth shape in the longitudinal direction; however, the width curve mostly showed a high-amplitude tooth shape and multi-fingering. This indicates the moderate–strong vertical and horizontal heterogeneity of the compound lava flow subfacies.

4.4. Heterogeneity Characteristics in Extrusive Facies

4.4.1. Heterogeneity Characteristics of Outer Zone Subfacies in Extrusive Facies

The lithology of the 4273–4281 m interval in Well X5 was trachyte, and the lithofacies was determined to be an outer zone subfacies. The mud logging indicated oil traces (Figure 9). The porosity spectra were mainly displayed in a very broad, multimodal spectrum with tails. There were multiple porosity bins. The VC showed moderate values, and the porosity width showed high values. These findings indicate that the pores in the outer zone subfacies are relatively dispersed, with moderate–strong vertical and horizontal heterogeneity.

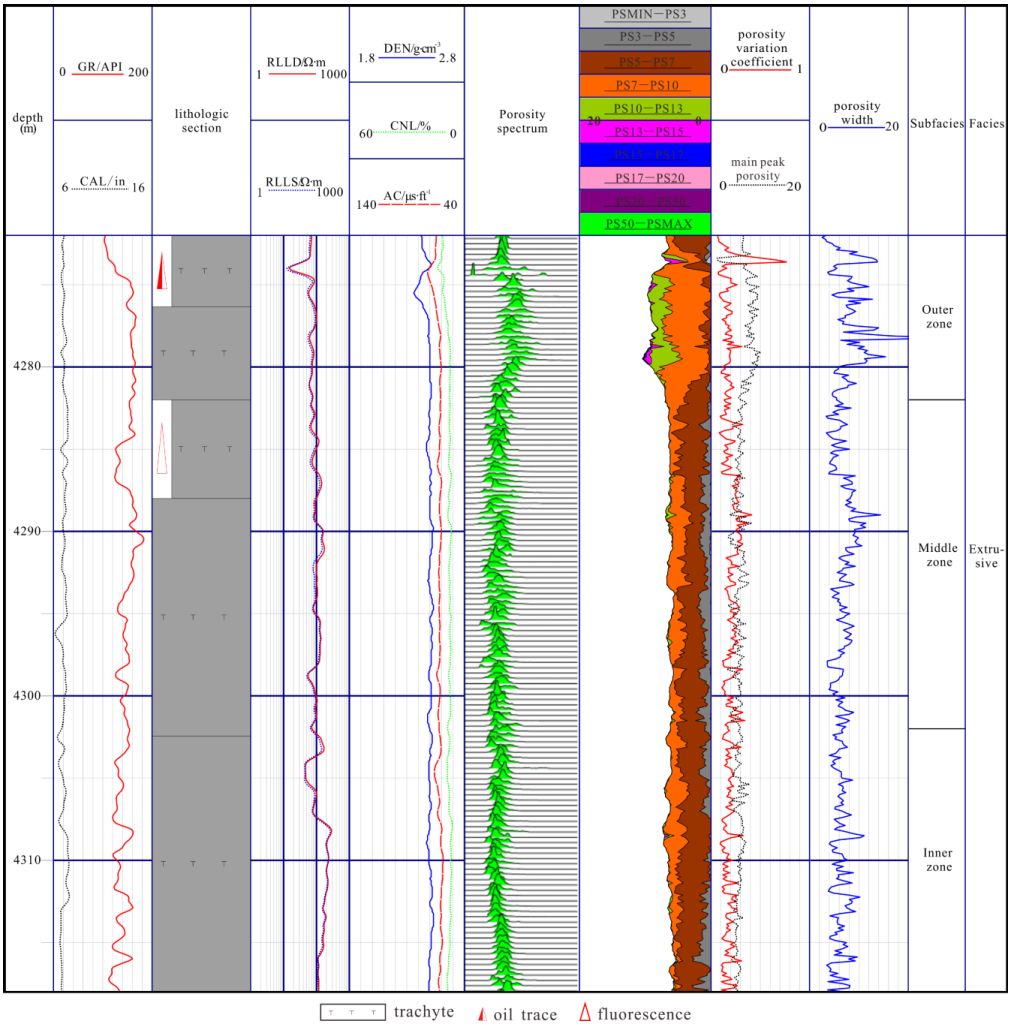

Figure 9. Heterogeneity characteristics of the extrusive facies in Well X5.

The porosity spectra analysis results manifested that most cases were characterized by a very broad, multimodal spectrum with tails (Figure 9). This hints that the porosity was less concentrated. The porosity encompassed a variety of porosity bins, and the main peak porosity was tooth-shaped. These results showed that the pores were not concentrated, leading to relatively strong vertical and horizontal heterogeneity. The VC was approximately 0.189, a moderate value; the porosity width was approximately 8.7, a high value. Moreover, the VC curve displayed a mostly moderate tooth shape in the longitudinal direction; however, the width curve showed a mostly high-amplitude tooth shape and multi-fingering. This indicates the moderate–strong vertical and horizontal heterogeneity of the outer zone subfacies.

4.4.2. Heterogeneity Characteristics of Middle Zone Subfacies in Extrusive Facies

The lithology of the 4282–4302 m interval in Well X5 was trachyte, and the lithofacies was determined to be a middle zone subfacies. The mud logging indicated fluorescence (Figure 9). The porosity spectra were mainly displayed in a broad, bimodal spectrum with tails. The porosity bins were diverse. The VC and porosity width showed moderate values. These findings indicate that the pores in the middle zone subfacies are less concentrated, with moderate vertical and horizontal heterogeneity.

The results of the porosity spectra analysis showed that most cases were characterized by a very broad, bimodal spectrum with tails (Figure 9). This hints that the porosity was less concentrated. The porosity interval contained a variety of porosity bins, and the main peak porosity was tooth-shaped. These results demonstrated that the pores were not concentrated, leading to moderate heterogeneity. The VC was approximately 0.212, and the porosity width was approximately 6.8, both showing moderate values. Moreover, the VC and the width curves mostly displayed a tooth shape in the longitudinal direction. These findings indicate the moderate vertical and horizontal heterogeneity of the middle zone subfacies.

4.4.3. Heterogeneity Characteristics of Inner Zone Subfacies in Extrusive Facies

The lithology of the 4302–4318 m interval in Well X5 was trachyte, and the lithofacies was determined to be an inner zone subfacies. The mud logging indicated no oil or gas presence (Figure 9). The porosity spectra were mainly displayed in a unimodal distribution with tails. The porosity bins were concentrated. The VC showed moderate values, and the porosity width showed low values. These indicate that the pores in the inner zone subfacies are concentrated, with weak vertical and horizontal heterogeneity.

The porosity spectra results analysis revealed that most cases were characterized by a unimodal distribution with tails (Figure 9). This hints that the porosity was concentrated. The porosity bins showed that PS5–PS7 accounted for over 70%, and the main peak porosity was approximately 5.6%, which is within the main bin. These results showed that the pores were concentrated, leading to relatively weak heterogeneity. The VC was approximately 0.174, showing a moderate value, and the porosity width was approximately 6.0, showing a low value. Moreover, the VC curve mostly displayed a low tooth shape in the longitudinal direction; however, the width curve showed a mostly low-amplitude tooth shape and multi-fingering. These findings indicate the weak–moderate vertical and horizontal heterogeneities of the inner zone subfacies.

5. Discussion

5.1. Analysis of Pore Characteristics and Favorable Reservoirs in Different Volcanic Facies

The volcanic facies provided a comprehensive reflection of the eruption mode and diagenetic process, which played a decisive role in the formation of the primary reservoir space and the transformation of the secondary reservoir space [33]. The reservoir space was complex and variable, and its heterogeneity was strong. Therefore, it was also the main factor influencing reservoir heterogeneity.

The diatreme subfacies were mainly formed through the stacking of pyroclastic rock and volcanic lava. The intergranular pores and fractures were developed, making it easy for the fluid to enter the reservoir. Later, dissolution transformation occurred, forming dissolution pores with a relatively uniform pore size (Figure 10a). Therefore, the VC showed a low value, and the porosity with showed a moderate value, because there were small pores in the primary reservoir space. The subfacies showed favorable reservoir properties and relatively weak heterogeneity.

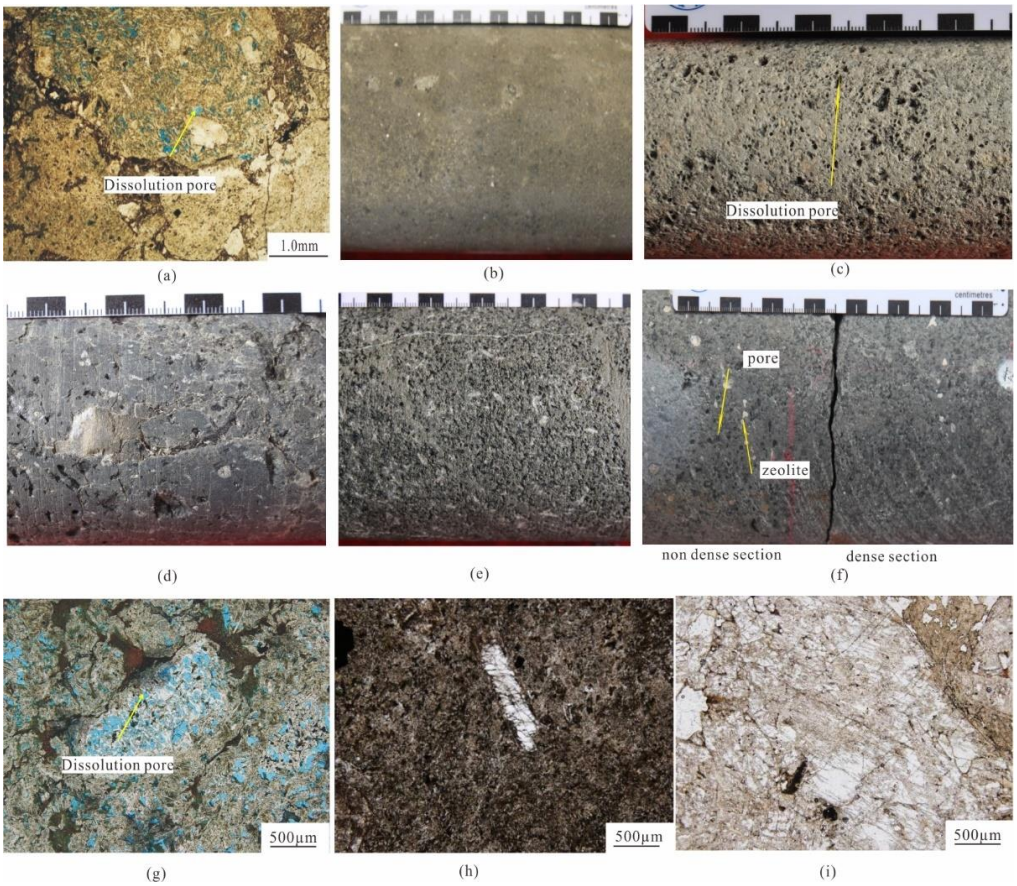

Figure 10. Typical core and thin section characteristics of different volcanic subfacies. (**a**) Diatreme subfacies, where blue represents the injected colloid. (**b**) Pyroclastic surge subfacies, crystal tuff, where breccia can be seen. (**c**) Pyroclastic flow subfacies, where dissolution pores were highly developed. (**d**) Hyaloclastite subfacies with brecciated basalt and a vitriclastic texture. (**e**) Tabular flow subfacies with coarse-grained basalt and a massive texture. (**f**) Compound flow subfacies with vesicular basalt in which the vesicles are filled with zeolite. (**g**) Outer zone subfacies, where the blue represents the injected colloid and dissolution pores were highly developed. (**h**) Middle zone subfacies with trachyte, a porphyritic texture, and massive structure. (**i**) Inner zone subfacies with trachyte and a massive structure.

The pyroclastic surge subfacies was mainly composed of rock debris/crystalline tuff (Figure 10b) with a fine grain size, dense reservoir, and low porosity. Therefore, the VC and porosity width presented low values. The reservoir was dominated by small pores. Although the overall heterogeneity was weak, favorable reservoirs could not easily form. The pyroclastic flow subfacies were formed after the rapid transportation and sedimentation of various volcaniclastic materials produced through explosive volcanic eruptions. These pores were similar to the primary pores of the diatreme subfacies but more prone to later dissolution and transformation and were more uniform (Figure 10c). Therefore, the VC showed a low value, and the porosity with showed a moderate value because there were

small pores in the primary reservoir space. These values were lower than those of the diatreme. The subfacies was also a favorable reservoir with good reservoir properties and weak heterogeneity.

The hyaloclastite subfacies was formed via magma emplacement underwater. The lithology was mostly brecciated basalt with a glassy structure (Figure 10d). The reservoir space was mainly composed of pores and contraction joints. The pore size varied greatly, and the pore heterogeneity was strong, making it difficult for oil and gas reservoirs to form. The pores of the upper and lower tabular flow subfacies were developed, and pores of different sizes were observed with strong heterogeneity. The reservoir was dense, with few pores in the middle (Figure 10e) and weak heterogeneity. Therefore, effective reservoirs could form in the upper and lower parts, but the thickness of the layers was relatively low, resulting in a limited mining value at present. The compound lava flow subfacies was formed through the accumulation of multiple intertwined lava flows, and overall, our analysis showed interactive characteristics of the porous zones and less porous/dense zones, with strong heterogeneity (Figure 10f). The pore size of the porous zone was also different, and the heterogeneity was strong. The reservoir developed with large pores, but some pores were filled with zeolite, leading to smaller pores (Figure 10f). Therefore, the VC showed a moderate value, and the porosity showed a high–moderate value because there were some large pores filled with zeolite. For a favorable reservoir to form in this subfacies, the heterogeneity performance would have to be moderate or low, and the vertical connectivity would have to be good. In addition, the strong heterogeneity of the subfacies was not conducive to the migration of oil into the reservoir, but it provided an opportunity to form a high-yield natural gas reservoir via easy natural gas migration.

The three subfacies of the extrusive facies are mostly continuously distributed. The outer zone was in contact with other strata, and the matrix and phenocrysts near the contact surface are prone to strong corrosion transformation. The dissolution pores are developed, and the pore sizes are also different (Figure 10g); thus, the heterogeneity is the strongest among the three types of subfacies. From the outer zone to the middle zone and the inner zone, the dissolution process weakens, and the development of primary pores decreases, leading to a gradual decrease in heterogeneity (Figure 10h,i). Therefore, the most favorable subfacies are the outer zone.

The above analysis of the pore characteristics was combined with the results regarding the heterogeneity of the different facies based on the electrical imaging log. This paper includes the heterogeneity characteristics and parameters of the different facies (Table 1). The authors previously classified the different volcanic rocks in terms of heterogeneity according to their porosity spectra, porosity bins characteristics, and VC. On this basis, the heterogeneity of volcanic facies can also be classified (Table 1), although there are some issues with this classification.

5.2. Heterogeneity Classification of Different Volcanic Facies

The results reflect the heterogeneity of different facies in detail based on the electrical imaging porosity spectrum, porosity bin, VC, and porosity width. Based on these characteristics and parameters, a simple classification can be carried out. However, the VC and porosity width cannot quantitatively classify heterogeneity when the VC is small, reflecting weak heterogeneity, and the porosity width is large, reflecting strong heterogeneity in a subfacies. Moreover, the two parameters cannot match, as in the case of the diatreme; pyroclastic flow subfacies with a low VC and a moderate porosity width; hyaloclastite; a compound lava flow; and outer zone subfacies with a moderate VC and high porosity width. The smaller the VC and the porosity width are, the weaker the heterogeneity is. Therefore, this paper proposes a new parameter, VC × porosity width (Pvcd):

$$\phi_{VW} = \phi_{VK} \times \phi_{WK} \tag{7}$$

The smaller the value is, the weaker the heterogeneity is, and vice versa. On the basis of this parameter, the heterogeneity performance of the nine subfacies is well-distinguished (Figure 11, Table 2).

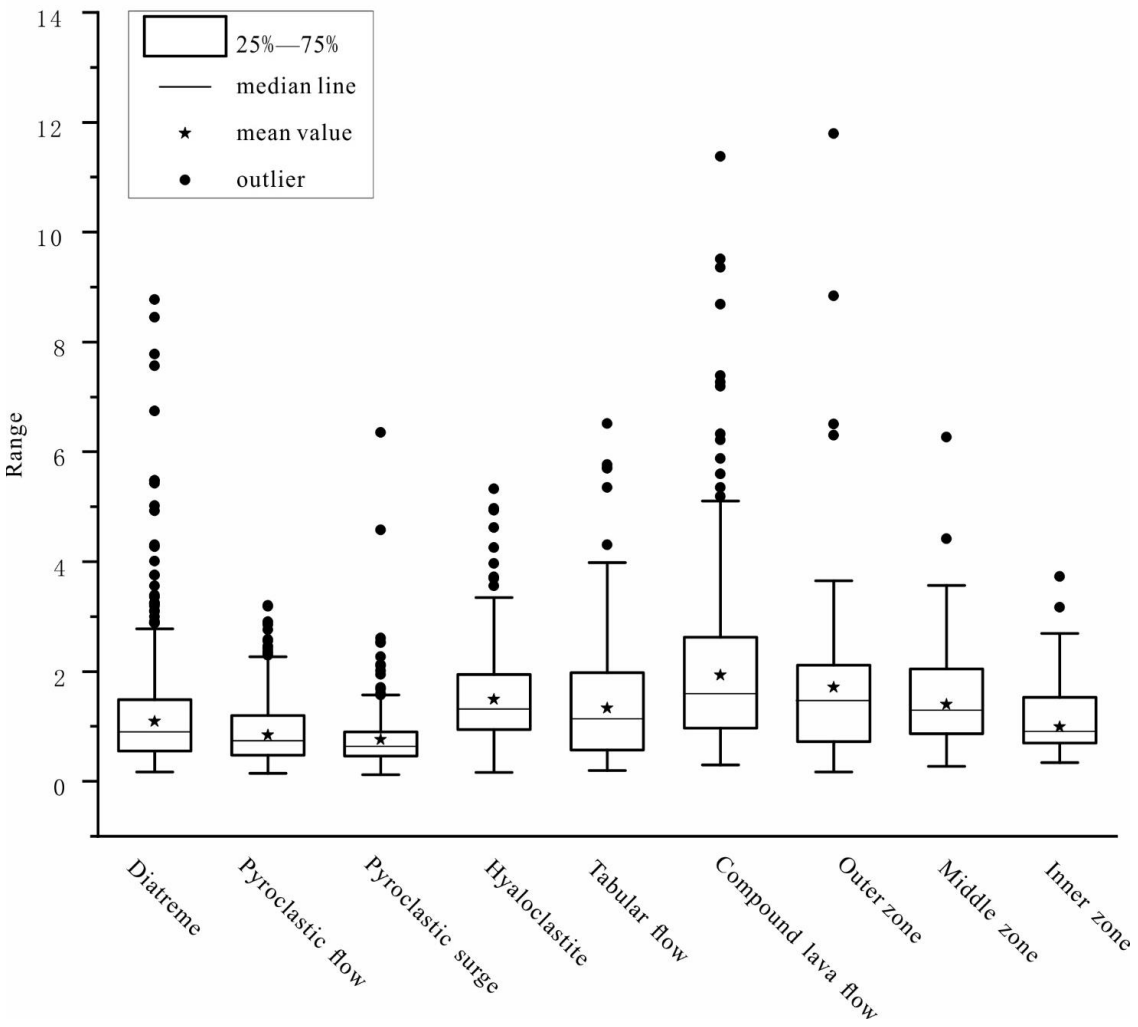

Figure 11. New heterogeneity parameter characteristics of different volcanic lithofacies.

Table 2. Heterogeneity characteristics and parameters of different facies.

Facies	Subfacies	Depth	Variation Coefficient	Porosity Width	Porosity Spectrum	Porosity Bin	VC × Porosity Width	Type
volcanic conduit	diatreme	4550–4583 m	0.131	8.4	unimodal	concentrated	1.100	I
explosive	pyroclastic surge	4440–4465 m	0.144	5.3	unimodal	concentrated	0.763	I
	pyroclastic flow	4450–4478 m	0.104	8.2	unimodal	concentrated	0.853	I
effusive	hyaloclastite	3802–3835 m	0.166	9.0	bimodal with tails, broad	less concentrated	1.494	II
	tabular flow	3825–3845 m	0.186	7.2	bimodal with tails	less concentrated	1.339	II
	compound lava flow	3811–3840 m	0.17	11.4	multimodal with tails	scattered	1.938	III

Table 2. *Cont.*

Facies	Subfacies	Depth	Variation Coefficient	Porosity Width	Porosity Spectrum	Porosity Bin	VC × Porosity Width	Type
extrusive	outer zone	4273–4281 m	0.189	9.1	multimodal with tails	scattered	1.720	III
	middle zone	4382–4302 m	0.212	6.8	bimodal with tails, broad	less concentrated	1.442	II
	inner zone	4302–4318 m	0.174	6.0	unimodal, narrow	concentrated	1.044	I

Based on the new parameters, drawing on the classification of lithological heterogeneity and considering the heterogeneity characteristics of different lithofacies, a heterogeneity classification standard for different lithofacies was established (Table 3). The classification results give priority to the new parameters, which can effectively classify heterogeneity. Based on these parameters, combined with the analysis in Section 5.1, the favorable lithofacies in the study area were identified, including the diatreme subfacies with medium or low heterogeneity, the pyroclastic flow subfacies with low heterogeneity, the compound lava flow subfacies with medium or low heterogeneity, and the outer zone subfacies with strong heterogeneity.

Table 3. Classification standards for volcanic rock reservoir heterogeneity in different facies.

Type	VC × Porosity Width	VC	Porosity Width	Porosity Spectrum	Porosity Bin	Evaluation
I	<1.1	<0.15	<6	unimodal, narrow	concentrated	weak
II	1.1~1.6	0.15~0.25	6~9	bimodal with tails, broad	less concentrated	moderate
III	>1.6	>0.25	>9	multimodal with tails, very broad	scattered	strong

6. Conclusions

The characteristics of the porosity spectrum, such as the number of peaks, the width, and the tail, can hint at the heterogeneity of the subfacies, and the distribution of porosity bins can also reflect heterogeneity. Both can qualitatively reflect heterogeneity. The new parameter, i.e., the variation coefficient × porosity width, VC, and the porosity width can be drawn upon to quantitatively characterize the heterogeneity of different lithofacies, which is useful for the effective evaluation of volcanic reservoirs.

On the basis of these three heterogeneity parameters, different lithofacies were divided into three heterogeneity categories: weak (I), moderate (II), and strong (III). For weak heterogeneity, with a P_{vcd} < 1.1, a VC < 0.15, and a porosity width < 6, the porosity spectra are focused in a unimodal distribution, and the porosity bins are concentrated. For moderate heterogeneity, with a P_{vcd} of 1.1–1.6, a VC of 0.15–0.25, and porosity width of 6–9, the porosity spectra are focused in a bimodal distribution with tails, and the porosity bins are less concentrated. For strong heterogeneity, with a P_{vcd} > 1.6, a VC > 0.25, and a porosity width > 9, the porosity spectra are focused in a multimodal distribution with tails, and the porosity bins are scattered.

Reservoir exploration efforts should give priority to diatreme subfacies with medium or low heterogeneity, pyroclastic flow subfacies with low heterogeneity, compound lava flow subfacies with medium or low heterogeneity, and outer zone subfacies with strong heterogeneity.

Author Contributions: Conceptualization, Z.L. and X.Z.; methodology, Z.L.; formal analysis, S.Z.; investigation, H.W.; data writing—original draft preparation, Z.L.; writing—review and editing, H.W. All authors have read and agreed to the published version of the manuscript.

Funding: This research was funded by the Joint Guiding Project of the Natural Science Foundation of Heilongjiang Province, grant number LH2023D008. This research was also funded by the Key Laboratory of Reservoir Formation Mechanism and Resource Evaluation of Heilongjiang Province Open Fund, grant number KL20190102.

Data Availability Statement: Not applicable.

Conflicts of Interest: The authors declare no conflict of interest.

References

1. Zou, C.; Zhao, W.; Jia, C. Formation and distribution of volcanic hydrocarbon reservoirs in sedimentary basins of China. *Pet. Explor. Dev.* **2008**, *35*, 257–271. (In Chinese with English Abstract) [CrossRef]
2. Yu, Y.; Xu, H.; Bai, Y. CT-based 3D pore-fracture network analysis of volcanic reservoirs of Lower Cretaceous Yingcheng formation in southern Songliao Basin, China: Impact on natural gas migration. *Geoenergy Sci. Eng.* **2023**, *223*, 211581. [CrossRef]
3. Tang, H.; Tian, Z.; Gao, Y. Review of volcanic reservoir geology in China. *Earth-Sci. Rev.* **2022**, *232*, 104158.
4. Bian, B.; Iming, A.; Gao, T.; Liu, H.; Jiang, W.; Wang, X.; Ding, X. Petroleum Geology and Exploration of Deep-Seated Volcanic Condensate Gas Reservoir around the Penyijingxi Sag in the Junggar Basin. *Processes* **2022**, *10*, 2430. [CrossRef]
5. Liu, Z.; Wang, Z.; Liu, J. The logging characteristics of the intermediate and mafic igneous rock from the depression in the Eastern Liaohe Basin. *Geophys. Prospect. Pet.* **2015**, *54*, 787–795. (In Chinese with English Abstract)
6. Han, R.; Wang, Z.; Guo, Y.; Wang, X.; Ruhan, A.; Zhong, G. Multi-label prediction method for lithology, lithofacies and fluid classes based on data augmentation by cascade forest. *Adv. Geo-Energy Res.* **2023**, *9*, 25–37. [CrossRef]
7. Nian, T.; Wang, G.; Cang, D. The diagnostic criteria of borehole electrical imaging log for volcanic reservoir interpretation: An example from the Yingcheng Formation in the Xujiaweizi Depression, Songliao Basin, China. *J. Pet. Sci. Eng.* **2022**, *208*, 109713. [CrossRef]
8. Ye, T. Lithofacies characteristics and controlling on volcanic reservoirs in the basement: A case study of the offshore Bohai Bay Basin, Eastern China. *J. Pet. Sci. Eng.* **2022**, *209*, 109860. [CrossRef]
9. Li, R.; Xiong, Z.; Wang, Z.; Xie, W.; Li, W.; Hu, J. Lithofacies Characteristics and Pore Controlling Factors of New Type of Permian Unconventional Reservoir in Sichuan Basin. *Processes* **2023**, *11*, 625. [CrossRef]
10. Jiang, F.; Cheng, R.H.; Ruan, B.T.; Lin, B.; Xu, Z.; Li, Z. Formation mechanism of volcanic reservoirs within a volcanostratigraphic framework: The case of the Wangfu fault depression in the Songliao Basin, China. *Mar. Pet. Geol.* **2017**, *84*, 160–178. [CrossRef]
11. Lu, X. Key factors controlling deep Carboniferous volcanic reservoirs in the east slope of Mahu Sag, Junggar Basin, NW China. *J. Pet. Sci. Eng.* **2023**, *220*, 111223.
12. Mao, Z.; Zhu, R.; Wang, J. Characteristics of Diagenesis and Pore Evolution of Volcanic Reservoir: A Case Study of Junggar Basin, Northwest China. *J. Earth Sci.* **2021**, *32*, 960–971. [CrossRef]
13. Fan, H.; Shi, J.; Fan, T. Sedimentary Microfacies Analysis of carbonate Formation Based on FMI and conventional Logs: A case study from the Ordovician in the Tahe Oilfield, Tarim Basin, China. *J. Pet. Sci. Eng.* **2021**, *203*, 108603. [CrossRef]
14. Wang, W.; La, W.; Fan, T. A Comparative Study on Microscopic Characteristics of Volcanic Reservoirs in the Carboniferous Kalagang and Haerjiawu Formations in the Santanghu Basin, China. *Front. Earth Sci.* **2021**, *9*, 735703. [CrossRef]
15. Huang, Y.; Hu, W.; Yuan, B.T. Evaluation of pore structures in volcanic reservoirs: A case study of the Lower Cretaceous Yingcheng Formation in the Southern Songliao Basin, NE China. *Environ. Earth Sci.* **2019**, *78*, 102. [CrossRef]
16. Sun, H.; Zhong, D.; Zhan, W. Reservoir characteristics in the Cretaceous volcanic rocks of Songliao Basin, China: A case of dynamics and evolution of the volcano-porosity and diagenesis. *Energy Explor. Exploit.* **2019**, *37*, 607–625. [CrossRef]
17. Nemes, I. Revisiting the applications of drainage capillary pressure curves in water-wet hydrocarbon systems. *Open Geosci.* **2016**, *8*, 22–38.
18. Schmitt, M.; Fernandes, C.; Neto, J. Characterization of pore systems in seal rocks using nitrogen gas adsorptioncombined with mercury injection capillary pressure techniques. *Mar. Petrol. Geol.* **2013**, *39*, 138–149. [CrossRef]
19. Xiao, D.; Lu, S.; Lu, Z. Combining nuclear magnetic resonance and rate-controlled porosimetry to probe the pore-throat structure of tight sandstones. *Pet. Explor. Dev.* **2016**, *43*, 961–970. [CrossRef]
20. Zuo, C.; Wang, Z.; Xiang, M.; Zhou, D.; Liu, Z. The radial pore heterogeneity of volcanic reservoir based on the porosity analysis of micro-electric imaging logging. *Geophys. Prospect. Pet.* **2016**, *55*, 449–454.
21. Liu, Z.; Wang, Z.; Zhou, D. Pore Distribution Characteristics of the Igneous Reservoirs in the Eastern Sag of the Liaohe Depression. *Open Geosci.* **2017**, *9*, 161–173.
22. Alizadeh, M.; Movahed, Z.; Junin, R. Porosity Analysis using Image Logs. *Environ. Sci.* **2015**, *10*, 326–337.
23. Fu, H.; Zou, C.; Li, N. A quantitative approach to characterize porosity structure from borehole electrical images and its application in a carbonate reservoir in the Tazhong Area, Tarim Basin. *SPE Reserv. Eval. Eng.* **2016**, *55*, 18–23.
24. Zhang, C.; Pan, B.; Zhang, X. Application of FMI logging data in evaluation of heterogeneity reservoirs. *Geophys. Prospect. Petrol.* **2011**, *50*, 630–633. (In Chinese with English Abstract)
25. Lai, J.; Pang, X.; Xiao, Q. Prediction of reservoir quality in carbonates via porosity spectrum from image log. *J. Petrol. Sci. Eng.* **2019**, *173*, 197–208. [CrossRef]

26. Ghasem, A.; Reza, M.; Ruhangiz, M. Reservoir heterogeneity and fracture parameter determination using electrical image logs and petrophysical data (a case study, carbonate Asmari Formation, Zagros Basin, SW Iran). *Pet. Sci.* **2020**, *17*, 51–69.
27. Li, X.; Zhou, Y.; Gou, Y. Porosity analysis of micro-electric imaging logging and its application in carbonate reservoir production capacity forecast. *J. Jilin Univ. (Earth Sci. Ed.)* **2012**, *42*, 928–934. (In Chinese with English Abstract)
28. Xie, H.; Wu, L.; Jiao, Y. The Quantitative Evaluation Index System for Uranium Reservoir Heterogeneity in Hantaimiao Region. *Ordos Basin. Earth Sci.* **2016**, *41*, 279–292.
29. Saeed, Y.; Ali, K.; Sirous, H. An integrated approach for heterogeneity analysis of carbonate reservoirs by using image log based porosity distributions, NMR T2 curves, velocity deviation log and petrographic studies: A case study from the South Pars gas field, Persian Gulf Basin. *J. Petrol. Sci. Eng.* **2020**, *192*, 107283.
30. Tadayoni, M.; Khalilbeyg, M.; Junin, R. A new approach to heterogeneity analysis in a highly complex carbonate reservoir by using borehole image and conventional log data. *J. Pet. Explor. Prod. Technol.* **2020**, *10*, 2613–2629. [CrossRef]
31. Liu, Z.; Wu, H.; Chen, R. Evaluation of volcanic reservoir heterogeneity in eastern sag of Liaohe Basin based on electrical image logs. *J. Pet. Sci. Eng.* **2022**, *211*, 110115. [CrossRef]
32. Mou, D.; Wang, Z.; Huang, Y. Lithological identification of volcanic rocks from SVM well logging data: Case study in the eastern depression of Liaohe Basin. *Chin. J. Geophys.* **2015**, *58*, 1785–1793. (In Chinese with English Abstract)
33. Huang, Y.; Shan, J.; Bian, W. Facies classification and reservoir significance of the Cenozoic intermediate and mafic igneous rocks in Liaohe Depression, East China. *Petrol. Explor. Dev.* **2014**, *41*, 734–744. [CrossRef]
34. Chu, Z. Structural Design for Micro-resistivity Scanner Imaging Logging Tool. *Well Logging Technol.* **1996**, *20*, 139–145. (In Chinese with English Abstract)
35. Lai, J.; Wang, G.; Fan, Z.; Chen, J. Sedimentary characterization of a braided delta using well logs: The upper Triassic Xujiahe formation in Central Sichuan basin, China. *J. Petrol. Sci. Eng.* **2017**, *154*, 172–193. [CrossRef]